Operation status and improvement of the integrated hybrid VRF system

Yusuke TOSAKA*[1], Shota HAGI[2], Tokimi KAWASE[3] and Tatsuo NOBE[1]

[1] Kogakuin University, Tokyo, Japan
[2] Taisei Corporation, Tokyo, Japan
[3]Yasui Architects & Engineers, Inc.
* *Corresponding author: dm20038@ns.kogakuin.ac.jp*

ABSTRACT

In recent years, the demand for energy conservation, the best energy mix, and thus air conditioning with energy options has increased. For this purpose, an integrated hybrid Variable refrigerant flow system (called hybrid VRF system) was developed in which a heat pump driven by a gas engine (GHP) and a heat pump driven by electricity are connected to the same refrigerant system. However, the actual characteristics of the hybrid VRF system remain unexplored. In this study, we analyzed a hybrid VRF system installed in a commercial facility. The results show that the actual operation differs from expectations. The results show that the GHP is preferentially operating when the system load factor is low, which is not optimal. Based on data obtained for indoor units, we propose a method to improve this problem.

INTRODUCTION

The energy used by buildings must be reduced. The Japanese oil crises in 1973 and 1976 and occurrences of large earthquakes have triggered the interest in energy conservation. Japanese nuclear power plants automatically shut down due to the Great East Japan Earthquake that occurred in 2011, leading to a power shortage in Japan. Therefore, Japanese people are interested in energy conservation.

In recent years, the construction of Zero Energy Buildings (called ZEBs), which can significantly reduce the annual energy consumption, has increased. Many energy-efficient buildings are constructed because the government enacted a law to subsidize ZEBs.

Therefore, the demand for energy conservation has increased. To satisfy this demand, an integrated hybrid VRF system has been developed (Furuhashi.Y, 2015).

In this study, we analyzed a hybrid VRF system installed in a commercial facility to determine its efficiency and energy consumption during actual operation. Based on the results, we propose operational improvements.

METHODS

Integrated hybrid VRF system

The hybrid VRF system is a multi-split air conditioner. This system connects the heat pump driven by a gas engine (GHP) and that driven by electricity (EHP) to the same refrigerant cycle. A remote monitoring server is used to operate the hybrid VRF system. The remote monitoring server sends driving instructions to the hybrid VRF system and the system sends driving data back to the remote server. By connecting the EHP and GHP to the same refrigerant cycle, the operating ratio of the GHP and EHP can be easily changed.

An integrated hybrid VRF system has two advantages. First, it can be operated with high efficiency. When the load factor is low, only the EHP operates. At a moderate load factor, only the GHP operates. When the load factor is high, the GHP and EHP operate simultaneously. Second, the electric power consumption can be reduced by combining the EHP and GHP, leading to a reduction in the electricity costs.

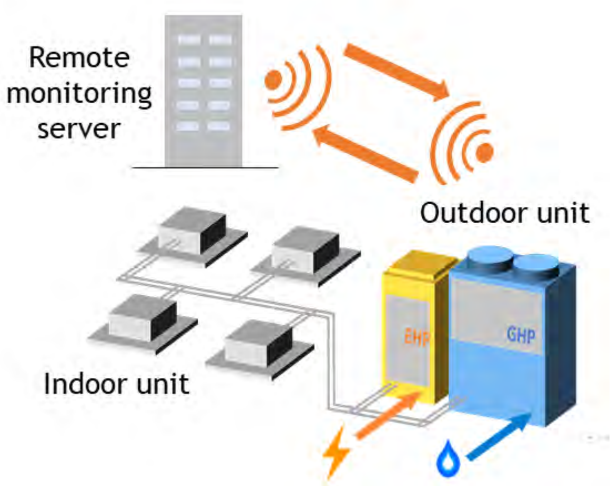

Figure 1. Schematic of the integrated hybrid VRF system

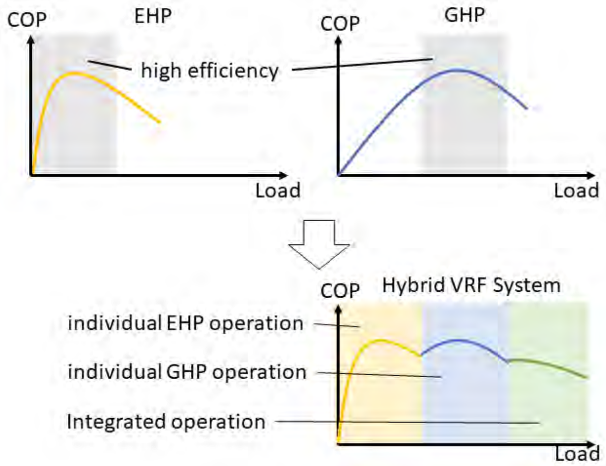

Figure 2. Illustration of the high-efficiency operation of the hybrid VRF

Measuring method

The air enthalpy method is commonly used to evaluate the performance of air-source heat pumps in Japan. Because the air enthalpy method is laboratory-based, it differs from the actual operation. Therefore, the multi-split measurement method (MM) was developed to measure the performance of outdoor units (Yasuda, M, 2015). The measurements in this study were performed using this method.

The MM method is based on the air enthalpy method. The heat exchange of the outdoor unit is calculated using the difference between the inlet surface and outlet surface temperatures as well as the wind speed. We installed a thermocouple and anemometer on the outlet surface of the outdoor unit and another thermocouple on the inlet surface to measure the temperatures and wind speed.

The differences between the inlet and outlet surfaces were determined as follows: The inlet surface was divided into four subsurfaces and the temperature of each subsurface was measured using a thermocouple. The temperatures were then weighted and the average temperature of the inlet surface was calculated. A thermocouple was installed on the outlet surface and the average temperature of the outlet surface was determined.

The inlet wind speed was measured based on a previously used procedure. In a previous study, we measured the relationship between the inlet and outlet wind speeds of the outdoor unit. Figure 3 shows the measurement points and Figure 4 shows the inlet and outlet wind speeds. The inlet surface was divided into subsurfaces and the wind speed was measured. The results show that the inlet and outlet wind speeds correlate and thus the inlet wind speed can be calculated from the outlet wind speed.

The inlet wind speed was calculated using Eq. (1):

$$V_n = \frac{V_{n.o}}{V_{out.o}} \times V_{out} = a_n \times V_{out}, \qquad (1)$$

where V_n is the inlet wind speed, $V_{n.0}$ is the base inlet wind speed, $V_{out.0}$ is the base outlet wind speed, and a_n is the ratio of the inlet wind speed to the outlet wind speed.

The heat exchange of the outdoor unit was calculated using Eq. (2):

$$Q = a_n \times V_n \times S_n \times \rho \times C_p \times (T_{in} - T_{out}), \qquad (2)$$

where Q is the amount of heat exchanged in each grid, S_n is the representative area, ρ is the specific weight, C_p is the specific heat, T_{in} is the inlet air temperature, and T_{out} is the outlet air temperature.

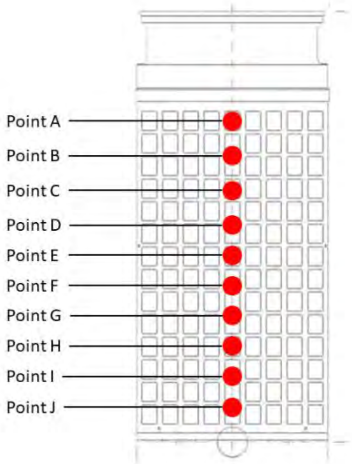

Figure 3. Points used for the measurement of the inlet wind speed

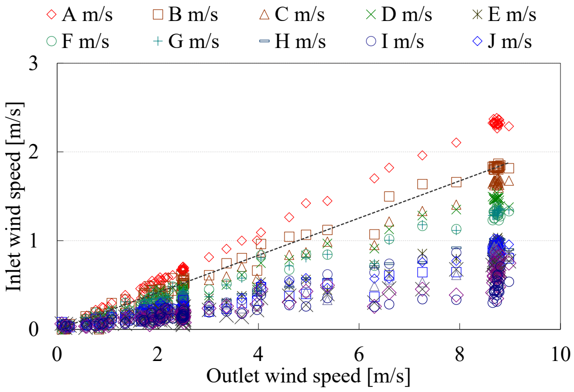

Figure 4. Outlet and inlet wind speeds

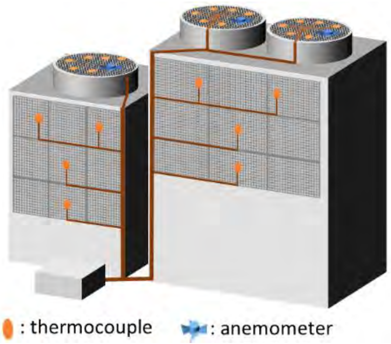

Figure 5. Schematic of the multi-split measuring method

Indoor unit data

It is important to analyze the operation of the indoor unit to determine the status of the entire system. Therefore, we obtained data for both the outdoor and indoor units. The data for the indoor unit, as listed in Table 1, were obtained from a hybrid VRF server. Both datasets were obtained in the same period.

Table 1. Indoor unit data

Date	Time	Set temperature	Inlet temperature	Mode
	Every 10 second	℃	℃	ON or OFF

Simulation method

To confirm the energy and cost reductions due the use of the hybrid VRF system, we simulated the energy consumption of a general EHP with the same horsepower as that of the hybrid VRF system. Table 2 provides an overview of the general EHP. We measured the long-term multi-split air conditioning performance. Based on the data, we calculated the average performance of the EHP (called standard EHP) (Yasuda.M, 2016). Figures 6 and 7 show the characteristics of the standard EHP. The amount of energy consumed was calculated using Eq. (3) and Figures 6 and 7:

$$\mathrm{COP} = \frac{P}{I}, \tag{3}$$

where COP is the coefficient of the performance of the outdoor unit, P is the heat production of the outdoor unit, and I is the dissipation power.

Actual measurement

Table 3 lists details about the study environment. The building in which we conducted the actual measurements was a commercial 6-story facility in Chiba, Japan. The measurements were conducted from August 1, 2019, to February 29, 2020. Table 4 lists information about the hybrid VRF system equipped with a GHP (45 kW) and EHP (22.4 kW).

Table 2. Information about the standard EHP

Cooling [kW]	Capacity	61.5
	Electric consumption	21.8
Heating [kW]	Capacity	69
	Electric consumption	25.7

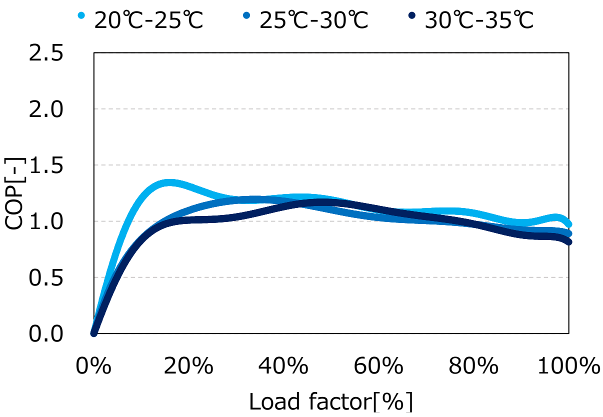

Figure 6. Standard EHP efficiency: cooling

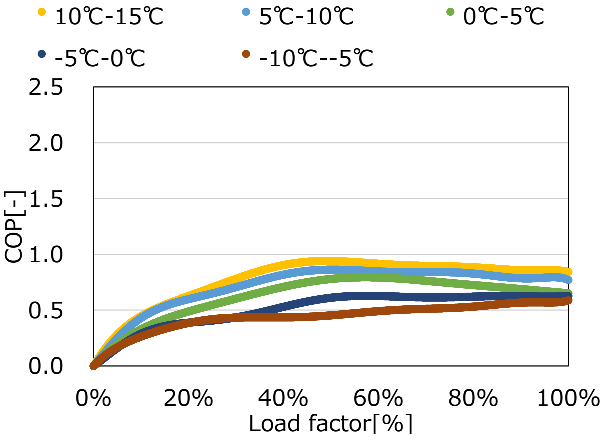

Figure 7. Standard EHP efficiency: heating

Table 3. Details about the study environment

Uses	Commercial construction
Location	Chiba, Japan
Floor	5 floors above ground
Measurement area	Ground floor
Measurement period	8/1/2019–2/29/2020

Table 4. Information about the hybrid VRF system

	Model	GHP	EHP
	HP	16	8
Cooling [kW]	Capacity	45	22.4
	Electric consumption	0.645	6.01
	Gas consumption	37.8	-
Heating [kW]	Capacity	50	25
	Electric consumption	0.505	6.53
	Gas consumption	34.9	-

RESULTS

Measurement results

Figure 8 shows the efficiency based on the relationship between the COP and load factor of the hybrid VRF system. Figure 9 shows the frequency of the cooling operation. As shown in Figure 8, the individual EHPs operated at a low load factor. The individual GHPs operated at a medium load factor. The most common load factor used for the operation was ~20%. The load factor almost never exceeded 60%. The operation of the EHP at a low load factor was highly efficient. As shown in Figure 8, the efficiency of the individual EHP operation at the low load was small. Even at a low load, many individual GHP and integrated operations were carried out.

Figure 10 shows the efficiency based on the correlation between the COP and load factor of the hybrid VRF system. Figure 11 shows the frequency of the heating operation. As shown in Figure 10, the COP increased as the load factor increased. Figure 11 shows that the EHP and GHP operated less during heating than during cooling.

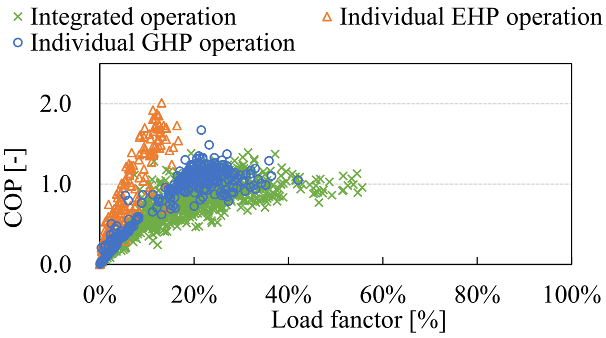

Figure 8. Efficiency of the hybrid VRF system: cooling

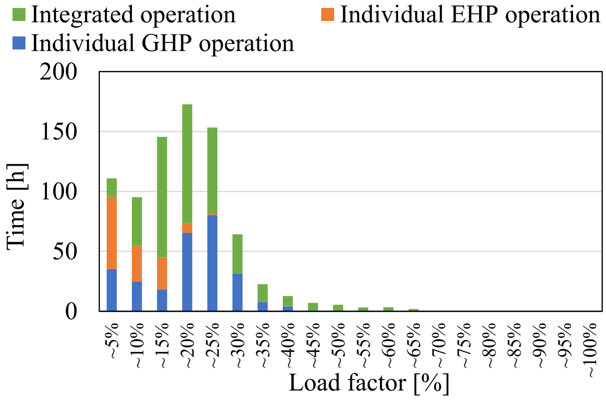

Figure 9. Frequency of the load factor: cooling

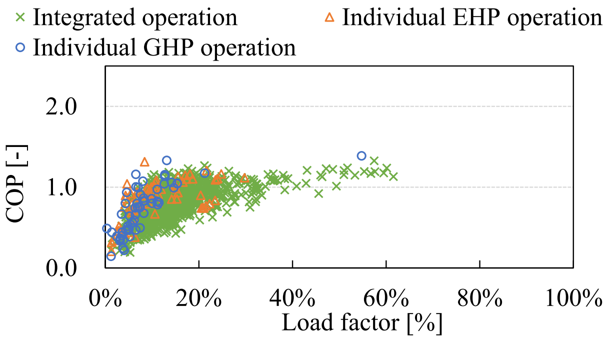

Figure 10. Efficiency of the hybrid VRF system: heating

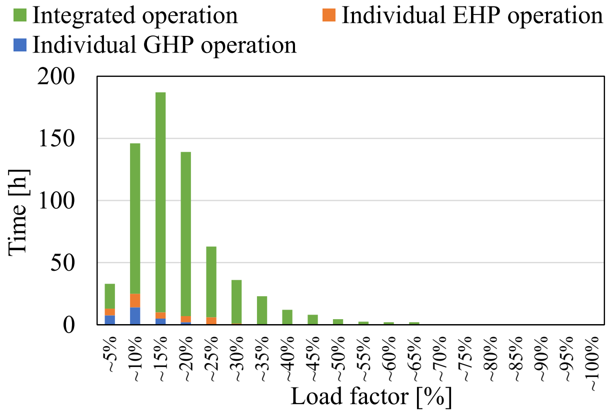

Figure 11. Frequency of the load factor: heating

Indoor unit analysis results

Figure 12 shows the operating ratio of the indoor units during the driving time. Figure 13 shows the correlation between indoor unit number and load factor during the operation. Table 5 lists the set temperatures of the indoor units. As shown in Figure 12, most of the time, only two indoor units were operating. Figure 13 shows that many EHP individually operated when only one unit was operating. However, when two or more indoor units were operating, many individual or integrated GHP operations were observed. As shown in Table 5, the set temperatures of unit Nos 1 and 4, which were always in operation, were lower than those of the other four units.

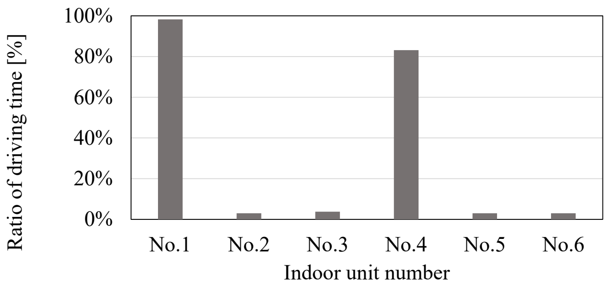

Figure 12. Operating ratio of indoor units

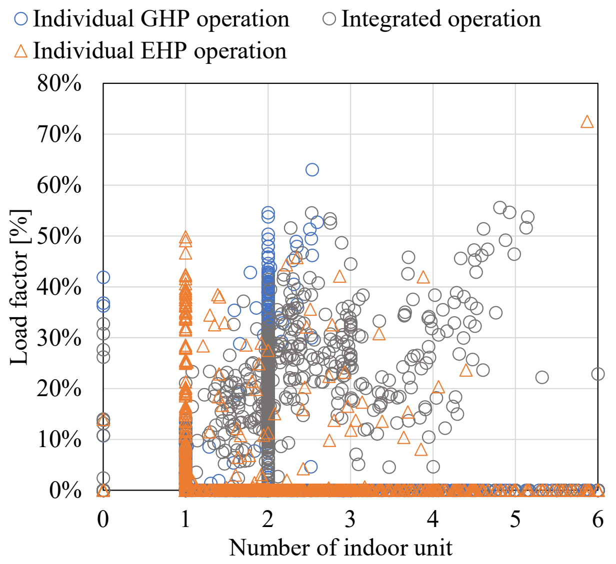

Figure 13. Correlations between the indoor units and load factor

Table 5. Set temperatures of the indoor units

Indoor unit number	1	2	3	4	5	6
Temperature of indoor unit	23	24	25	23	24	26

Simulation results

Figure 14 shows the energy consumptions of the hybrid VRF system and standard EHP. Figure 15 shows the monthly energy costs of the hybrid VRF and standard EHP systems. Based on the figure, the cooling operation from August to October using the standard EHP system consumed less energy than the operation of the hybrid VRF system. From December to February, the standard EHP consumed more energy than the hybrid VRF system. When the energy consumption was increased in all periods, the energy consumptions of the standard EHP and hybrid VRF systems remained the same. As shown in Figure 15, the costs of the hybrid VRF system are lower than those of the standard EHP, in all months.

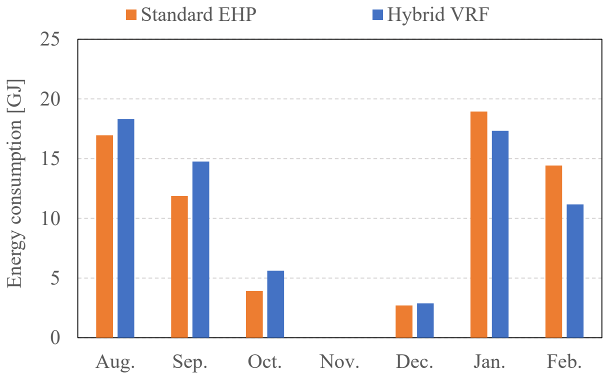

Figure 14. Comparison of the energy consumptions of the hybrid VRF system and standard EHP

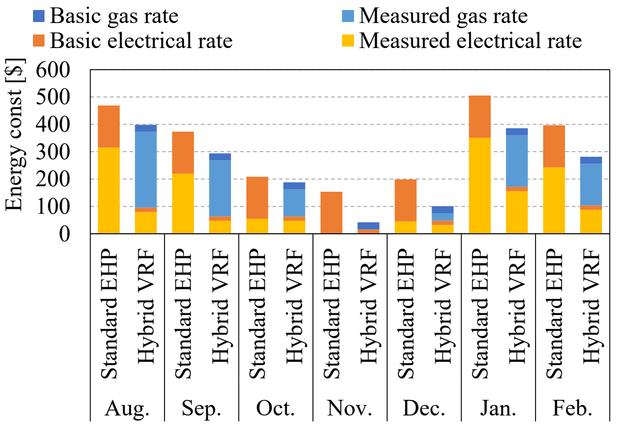

Figure 15. Energy costs of the hybrid VRF system and standard EHP

DISCUSSION

In this study, measurements were carried out to gain insights into the actual performance of the hybrid VRF system. Hagi et al. (2019) found that the individual EHP operation at a low load factor was big. but the results show that the efficiency of the individual EHP operation at a low load factor was small. To confirm the advantages of the hybrid VRF system, we compared it with a standard EHP system. The results show that the same amounts of energy were consumed. However, the costs of the hybrid VRF system were less than those of the standard EHP system.

The set temperature is the main cause of the inefficient operation of indoor units. The set temperatures of units Nos 1 and 4 were lower than those of Nos 2, 3, 5, and 6. Because the set temperature was low, only Nos 1 and 4 operated for a long time. In addition, when two or more indoor units were in operation, there was little EHP individual operation, which might be due to the difference in the set temperatures of the indoor units. Therefore, this problem could be solved by using the same set temperatures for all indoor units. Because the efficiency of the operation of an individual EHP is high, this measure will also lead to the reduction of the energy consumption.

In the future, measurements should be carried out under improved conditions.

CONCLUSIONS

In this study, measurements and simulations were conducted to study the performance of the hybrid VRF system. The comparison of the hybrid VRF system and standard EHP shows that the energy consumption of both systems is the same. The energy costs of the hybrid VRF system are lower than that of the standard EHP. However, the results show that the operation is not ideal. The results obtained for the indoor units indicate that the problem can be solved by using the same set temperatures for all indoor units.

REFERENCES

Furuhashi, Y et al. 2015. "A Study on the Hybrid Air-conditioning System having GHP and EHP in the Single Refrigerant Cycle Part 1 an Examination about the Most Optimal System Constitution by the Simulation" Proceedings of Society of Heating, Air-Conditioning and Sanitary Engineers of Japan. Osaka (Japan), 449-452 (Sep.)

Furuhashi, Y et al. 2015. "A Study on the Hybrid Air-conditioning System having GHP and EHP in the Single Refrigerant Cycle Part 2 Verification of the Effectiveness of the Optimal Control in an Actual Building" Proceedings of Society of Heating, Air-Conditioning and Sanitary Engineers of Japan. Kagoshima (Japan), 273-276 (Sep.)

Yasuda, M et al. 2015. "Study on simple on-site measurement method of VRF (Part 1) Proposal of measurement using Weighted Average method" Proceedings of Society of Heating, Air-Conditioning and Sanitary Engineers of Japan*. Osaka (Japan),* 185-188 (Sep.)

Yasuda, M et al. 2016. "Study on the average partial load characteristics extraction method in VRF system" Proceedings of Society of Heating, Air-Conditioning and Sanitary Engineers of Japan. Kagoshima (Japan), 265-268 (Sep.)

Hagi, S et al. 2019. "Operational status evaluation of integrated hybrid VRF in tenant office building" Proceedings of Society of Heating, Air-Conditioning and Sanitary Engineers of Japan. Sapporo(Japan), 241-244 (Sep.)